31st Congress of the International Council of the Aeronautical Sciences

Belo Horizonte, Brazil; September 09-14, 2018

ON THE CALIBRATION OF THE INTERMITTENCY TRANSITION TURBULENCE MODEL FOR WIND TURBINE AIRFOIL BY MACHINE LEARNING ALGORITHM

M Anas Abd Bari*, Andrea Da Ronch*, Marco Panzeri, Jernej Drofelnik***
*University of Southampton, Southampton, SO17 1BJ, UK.
** Noesis Solutions N.V., 3001 Leuven, Belgium.

Keywords: *intermittency turbulence model; machine–learning; wind turbine aerodynamics*

Abstract

Fully turbulent wind turbine computational fluid dynamics simulations have been shown to over-predict the aerodynamic performances. To ensure a correct prediction, modelling of flow transition from laminar to turbulent over the blade is becoming necessary. While several transitional turbulence models exist, the one equation intermittency γ model coupled with the k-ω SST turbulence model offers a simple framework against wide range of generic industrial application. However, the model is yet to be calibrated for certain cases especially for external aerodynamic flows at low turbulent intensity. In this paper, the epistemic uncertainty of several model constants related to the transitional triggering function is investigated using machine learning. The procedure is demonstrated for the S809 airfoil. It was found that: (a) some coefficients have a large impact on the results at high angles of attack, causing fluctuation of the results and (b) the calibration of the turbulence model is influenced by several factors, for instance, the solver limiters.

1 Introduction

Epistemic uncertainties are inherent to any computational model due to our lack of knowledge of some of the model parameters. The closure coefficients are a common source of epistemic uncertainty in a turbulence model. The model equations that are created to mitigate the closure problem contain coefficients which values are determined from calibration with experimental values [1]. It is for some of these so–called closure coefficients that a prior uncertainty interval is determined. Cruz et al. [2] for instance performed computational fluid dynamics (CFD) calculation with several turbulence models and found that a zero–equation model gives lower root mean square (RMS) error than a two–equation model. This is because the latter needs a few constants that are often fine–tuned for specific applications, thus showing that a standard turbulence model coefficients do not accurately represent the turbulence properties of the flow. Yarlanki et al. [3] also concluded that turbulence coefficients are usually approximated from simpler geometry and it is plausible that these coefficients need further calibration and the standard values may not work well. Sørensen et al. mentioned that:

> "Determining the empirical correlations by numerical optimization, along with debugging the model, demands a very large amount of computations, and it is the hope that other researchers can confirm the present expressions by implementation in other flow solvers [4]."

Upon reflection from this statement, it is therefore necessary to perform a fast technique to calibrate the turbulence model, in this case, machine

learning algorithm seems to satisfy the purpose as previously proved in [5]. In addition, the necessity to calibrate the intermittency transition model is explicitly mentioned in Ansys Documentation as followings:

> "The γ transition model has only been calibrated for classical boundary layer flows. Application to other types of wall–bounded flows is possible, but might require a modification of the underlying correlations [6]."

This model was evaluated previously by Colonia et al. [7] at Re larger than $1 \cdot 10^6$ by calibrating a certain parameter of the model. However a big loophole remains as a further complex calibration involving more model correlations are necessary by means of further reducing the uncertainty quantification in the CFD calculation.

The decision to calibrate the transitional rather than fully turbulence model for wind turbine application is explained here. Without incorporating the influence of transitional effect, the prediction of flow over the wind turbine blade will incur an over estimation of the total drag to an incorrect prediction of the blade load and performance. With that, the modelling of transitional flow from a laminar to fully turbulent boundary layer is essential since it can improve the accuracy and capability of CFD technique to simulate the actual physics of the flow field more realistically by exploiting the possible presence of laminar flow. By taking into account the transition process during the design phase of the blade, it may play a compelling role to maximize the aerodynamic performance at a specific operating condition without compromising its performance in a fully turbulent flow. Unlike the fully turbulent simulation, the performance is improved because the existence of the transition model could delay the transition to turbulence while maintaining the favourable pressure gradient, in turn reducing total drag [8]. This phenomenon was observed as simulated by Menter et al. [9] for 2D and 3D wind turbine cases by which the output torque of the turbine differs by 80% between the two approaches. This observation is one of the reasons that explains the necessity of using transition prediction models in CFD–based integrated design frameworks.

Nevertheless, this important effect is not included in most of current CFD simulations because the transitional modelling does not provide similar broad spectrum of CFD–compatible model formulations that exist as for the fully turbulent flow models. According to Menter and Langtry [10], there are two reasons that lead to this situation. Firstly, different applications have their specific mechanism to trigger the transition i.e natural, bypass or separation–induced separation. Secondly, the conventional Reynolds averaged Navier–Stokes (RANS) equations cannot be easily incorporated to the description of transitional flows in which the linear and non–linear effects are relevant. This is because of the difficulty to apply the transition process since RANS eliminates the effect of linear disturbance growth. Yet, much like in fully turbulence modelling, it is crucial to develop engineering models that can be applied in wide different application areas and accuracy requirements.

The transition prediction methods range from generic empirical approach utilizing the linear stability equation (LSE) such as the e^N approach [11, 12], to parabolic stability equation (PSE) and more recently the one equation intermittency, γ model [13] based on the earlier two equations Local–Correlation based Transition Modelling (LTCM) of $\gamma - \tilde{Re}_\theta$ [9, 14, 15]. According to Mayda and Van Dam [16], wind turbine blade typically operates at Reynold number, Re, on the order of 10^6. At this order, the airfoils are very sensitive to the Re thus the development of laminar separation bubbles is possible. Several works were conducted to accurately predict the location of transition. Windte et al. [17] and Lian et al. [18] for instance has utilized the e^N coupled with CFD to study the transition for 2D cases. Although the stability based methods were very successful in predicting the transition for many years, they are not compatible with general–purpose CFD methods as typically applied in complex geometries.

The reason is that these methods require a priori knowledge of the geometry and the grid topology. Due to this reason, Langtry and Menter [15] proposed a new two equations Local–Correlation based Transition Modelling (LTCM) by formulating a set of CFD–compatible transport equation which allow combining experimental correlations in a local fashion with underlying turbulence model. In the earlier version, two additional transport equations, one for the intermittency and the other for the transition onset correlation were defined. Sørensen [4] attempted to use this transition model coupled with RANS solver for a 2D wind turbine airfoil and full rotor configuration. Similar initiative was also conducted by Khayatzadeh and Nadarajah [8] and both showed promising results. In a more recent effort, while conserving the original feature of the original LTCM model, a simplified version was released by reducing the formulation to a single γ equation only. This updated model, while conserving the original LTCM feature was validated against generic turbomachinery and external aeronautical test cases by Menter et al. [13] for Re less than $500 \cdot 10^3$ and found good agreement with the available experimental data, and some of the coefficients were adjustable to allow for fine tuning of the model.

The work in this paper is build on two main objectives: 1) exploit machine learning algorithm as a fast technique to assess the sensitivity of the closure coefficients towards the output quantities of interest and 2) calibrate the closure coefficients of the one–equation intermittency transition turbulence model by reducing the discrepancies between the experimental data and numerical results for subsonic flow around S809 airfoil. The work, therefore, assumes that the experimental data provide a reasonable accuracy which can be used for calibration, and are error–free. This assumption may not be fully met, but the data set is the only one available. To exploit the availability of high–performance computer (HPC) facility, the numerical calculations were performed on the HPC of the University of Southampton known as Iridis4. In this paper, the constants that are directly influenced by the transition triggering function of the γ–equation model, are identified and calibrated for the S809 wind turbine airfoil, at Re=$2 \cdot 10^6$ at various angle of attacks. Through an approach based on machine learning techniques, a modification of the correlation to improve the results is presented and compared against the fully turbulent simulation and experimental data. The current initiative is to further calibrate the correlations by means of a machine learning–based adaptive design of experiments (ADOE) technique as similarly utilized and described by Da Ronch et al. [19] based on surrogate models. To perform the sensitivity analysis and the model calibration, a surrogate model resembling the dependency of the closure coefficients and the output quantities of interest is constructed. The crucial aspect of this methodology is to maintain an accurate representation of the system behavior with a very minimum number of CFD simulations, explaining the key attribute of the ADOE.

A description of the flow solver and the machine–learning methodology to calibrate the closure coefficients of the intermittency turbulence model is presented in Section 2. A comprehensive formulation of the model as well as the required necessary modifications to both the transition and the underlying k–ω SST turbulence model is included. Then Section 3 introduces the test case used in the current study and the findings are presented. Finally, Section 4 denotes the conclusions as well as future recommendations.

2 Methodology

Two computational software are used in the framework. Firstly, the aerodynamic calculations are performed by commercial CFD software ANSYS Fluent and the description of the intermittency turbulence model is also included in Section 2.1. Section 2.2 briefly discussed the calibration of the closure coefficients by the software Noesis Optimus [20].

2.1 Flow Solver

ANSYS Fluent was chosen to demonstrate the consistent integration of the ADOE with a well–established CFD tool. The incompressible fluid is solved by finite volume pressure based solver. SIMPLE pressure–velocity coupling scheme was chosen to solve the transition turbulence model coupled with the k–ω SST. The pressure is discretised by second order. The spatial discretisation of the momentum, turbulent kinetic energy and specific dissipation rate are specified to second order upwind accuracy.

2.1.1 *Turbulence Model Formulation*

For detailed explanation of the intermittency turbulence model, the reader is referred to Menter et al. [13] by which the definition of the notations used and equations mentioned in this work are maintained as in the reference. The transport equation for the intermittency γ transition model is given as:

$$\frac{\partial(\rho\gamma)}{\partial t}+\frac{\partial(\rho U_j\gamma)}{\partial x_j}=P_\gamma-E_\gamma+\frac{\partial}{\partial x_j}\left[\left(\mu+\frac{\mu_t}{\sigma_y}\right)\frac{\partial\gamma}{\partial x_j}\right] \tag{1}$$

The transition source term, P_γ, is a function of a correlation in the form of critical momentum thickness Reynolds number, $Re_{\theta c}$, given as follow

$$Re_{\theta c}(Tu_L,\lambda_\theta)=C_{TU1}+C_{TU2}\,e^{(-C_{TU3}\,Tu_L\,F_{PG}(\lambda_\theta))} \tag{2}$$

The minimal value of the $Re_{\theta c}$, is determined by the constant C_{TU1} whereas its maximal value is controlled by the sum of C_{TU1}+C_{TU2}. The C_{TU3} constant defines the rate of decay of the $Re_{\theta c}$ as the turbulence intensity, Tu increases. The subscript L in the equation denotes the local value of the respective parameter. To incorporate the transition effect to the streamwise pressure gradient, the constant F_{PG} is introduced and reads as

$$F_{PG}(\lambda_{\theta L})=\begin{cases}\min(1+C_{PG1}\lambda_{\theta L},\ C_{PG1}^{lim}), & \text{for } \lambda_{\theta L}\geq 0.\\ \min(1+C_{PG2}\lambda_{\theta L}+C_{PG3}\ \min[\lambda_{\theta L}+0.0681,\ 0],C_{PG2}^{lim}), & \text{for } \lambda_{\theta L}<0.\end{cases} \tag{3}$$

The value of $Re_{\theta c}$ is adjusted in the favorable and adverse pressure gradients regions by the constants C_{PG1} and C_{PG2}, respectively. In order to correct the $Re_{\theta c}$ in separation region, C_{PG3} is included. From Eq. 2, it is clear that the $Re_{\theta c}$ depends on the pressure gradient parameter, λ_θ. In the coupling with the SST turbulence model, an additional term, P_k^{lim}, in Eq. 4 was introduced into the turbulent kinetic energy production term (k–equation) to ensure the transition process is more reliable when it is developing under low Tu or/and when it starts in a separation bubble. The 'max$(3C_{sep}\mu-\mu_t,0)$' switches this additional term off when the transition process is completed and the boundary layer is in fully turbulent state when the turbulent viscosity, $\mu_t > 3C_{sep}\mu$.

$$\begin{aligned}P_k^{lim}&=5C_k\,\max(\gamma-0.2,0)(1-\gamma)\\ &F_{on}^{lim}\max(3C_{sep}\mu-\mu_t,0)S\Omega\end{aligned} \tag{4}$$

In addition, the triggering transition function relies on the vorticity Reynolds number, Re_v rather than $Re_{\theta c}$ as in Eq.(4) of Menter et al. [13] or similarly given as

$$F_{onset}=\frac{Re_v}{2.2\,Re_{\theta c}} \tag{5}$$

The strong effect of the pressure gradient can be incorporated by calibrating the 2.2 factor of this equation as shown by Colonia et al. [7], or through the correlations of Eq. 2 and Eq. 3. According to Menter et al. [13], the latter approach is more favorable.

Epistemic Interval Based on previous studies, 7 parameters having correlation to the transition equations have been identified herein, namely the C_{TU1}, C_{TU2}, C_{TU3}, C_{PG1}, C_{PG2}, C_{PG3}, and C_{SEP}, and will be calibrated in the present work through the machine learning technique. One of the is-

sues encountered was to identify the appropriate range for these constants for the calibration. According to Menter et al.[13], it is given that the value of F_{PG} is always positive while the constant C_{PG1}^{lim} and C_{PG2}^{lim} are equal to 1.5 and 3.0 respectively. With this information, the suitable range of C_{PG1} and C_{PG2} for -0.1$\leq \lambda_\theta \leq$ 0.1 can be determined from Eq. 3. Another proposed modification is to rescale the value of C_{TU1} and C_{TU2}. According to the Tollmien–Schlichting limit of stability, the minimum value of $Re_{\theta c}$ is 163, which is directly related to the constant C_{TU1} [21]. Hall [22] on the other hand, suggested that this value should be 320.0. In order to determine the range of C_{TU2}, the reader is referred to Fig. 1 similarly found in [21]. At given Tu level as prescribed in the experimental procedure, the range of $Re_{\theta c}$ can be determined. For instance, at 0.02% Tu level, the value of $Re_{\theta c}$ varies between 1150 to 3000. With known lower and upper limits of all of the other constants in Eq. 2 apart from the C_{TU3}, the range of this parameter can be determined. The nominal value and limits of these constants are summarized in Table 1.

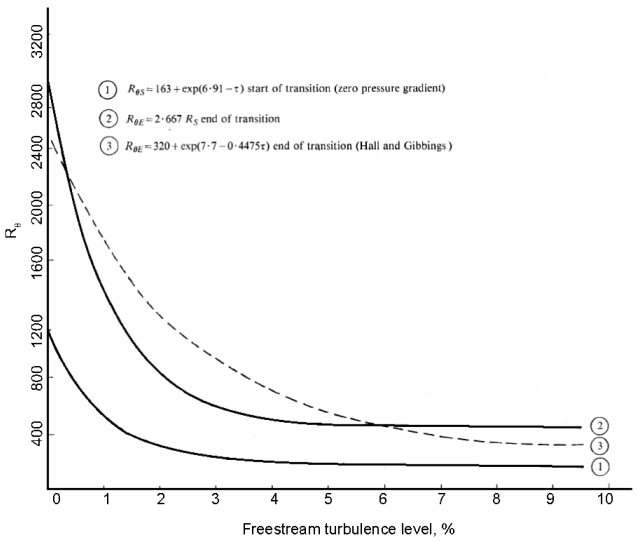

Fig. 1 Momentum thickness Reynolds number at start ($R_{\theta S}$) and end ($R_{\theta E}$) of transition for zero pressure gradient, reproduce from [21].

2.2 Machine–learning Technique

The Noesis Optimus software platform provides an iterative adaptive DOE methodology strongly based on machine learning techniques. The ADOE entails three main steps: 1) the regions in the design space that are difficult to model are identified; 2) The design points in those area are distributed iteratively; and 3) the surrogate model that best fits the results obtained from design of experiment (DOE) plan is selected automatically. The strategy used is to build designs of experiments that is based on an explicit trade–off between reduction in global uncertainty and exploration of regions of interest. This framework analyses the data history to distribute the design points of the next iterations in areas of the parameters space considered of interest. Two opposite factors determine the choice of new sample for the design points namely the space–learning and feature–learning. The objective of the space–learning is to explore the new design space and filling it uniformly without considering any information about the response of the model. The feature–learning is used to improve accuracy of the surrogates of critical areas of the design space by adding new samples in those area. The driven factor that determine reliability of the machine–learning approach adapted by Noesis Optimus is the capability to identify the best possible surrogate models for a given set of design points. The surrogate models identified by the ADOE are then employed to efficiently evaluate the sensitivity of the turbulence model closure coefficients towards the aerodynamic features and then calibrate the values of these coefficients based on the experimental data. For further detail of this machine–learning framework, the reader is referred to Da Ronch et al. [19].

3 Test Case & Results

3.1 S809 Airfoil

The S809 airfoil is used for the uncertainty quantification and calibration of the intermittency turbulence model. This airfoil was chosen herein as it was constructed specifically for wind turbine

Table 1 Nominal value and epistemic interval for the turbulence constant at Tu=0.02% and -0.1$\leq$ $\lambda_\theta \leq$ 0.1.

Constant	Nominal Value	Lower Limit	Upper Limit
C_{TU1}	163.00	100.00	320.00
C_{TU2}	1002.25	1000.00	2650.00
C_{TU3}	1.00	0.00 or 1.00	
C_{PG1}	14.68	-100.00	50.00
C_{PG2}	-7.34	-10.00	6.00
C_{PG3}	0.00	0.00 or 1.00	
C_{SEP}	1.00	0.00 or 1.00	

application. This 21%–thick airfoil was designed and analysed theoretically and experimentally at the low–turbulence wind tunnel of the TU Delft at Re=1–3.0·10^6 for a series of angle of attack, α=-17.1–20.4 deg [23].

In this case, the simulation was conducted at Re=$2 \cdot 10^6$ with six α equal to -0.01, 5.13, 9.22 deg, 11.22, 15.2 and 16.2 deg. The computational domain is depicted in Fig. 2. The medium grid was chosen after a grid convergence study was conducted to ensure the independence of the results with the current grid size. The computed C_L for all three level of grids is depicted in Table 2. In this table, Δ% is the percentage difference between the computed and experimental value. It is shown that the change of C_L between the fine and medium grid is less than 0.2% which indicate that further refinement of the grid is not necessary. The C–domain consists of 24,896 nodes with 192 nodes around the airfoil and 34 nodes in the normal direction in a single block. The y^+ is well below 0.5 along the airfoil chord and the farfield is located at a distance of 50 chords away from the airfoil. All the calculations used the pressure–based solver with SIMPLE pressure–velocity coupling scheme. The spatial discretisation of the pressure is based on second order accuracy whereas the momentum, turbulent kinetic energy and specific dissipation rate are discretised by second order upwind accuracy. The boundary condition for the inlet and outlet is specified as velocity–inlet and pressure–outlet respectively. A no–slip wall boundary condition was applied on the airfoil surface.

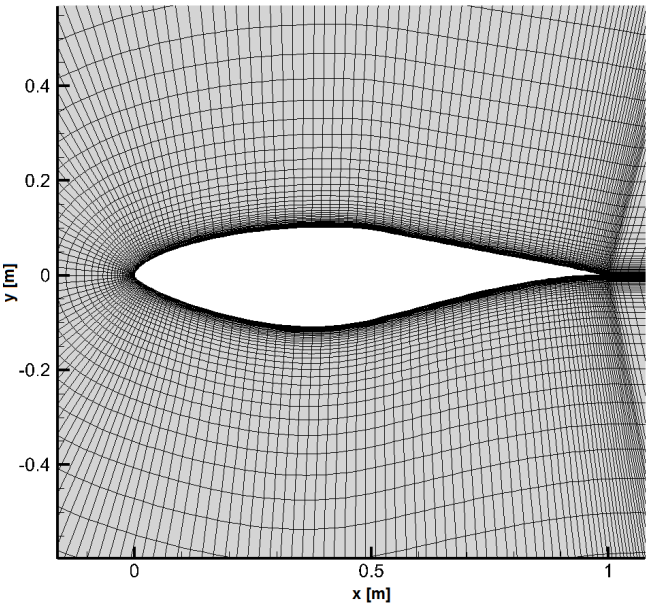

Fig. 2 Medium grid for the S809 airfoil.

A preliminary study was conducted to ensure the results are fully converged. Two flow conditions were chosen at 5.13 and 11.22 deg angle of attack. The simulations were conducted for 30,000 iterations with check points at every 10,000 iterations. The lift coefficient, C_L, was compared at these intermediate points. In Fig. 3, the convergence of the C_L with the number of iterations is shown in which the vertical dashed lines indicate the check points. In Table 3, the C_L at these check points are presented. It was found that as the number of iterations exceeding 10,000, the difference of the C_L discrepancy is well below 0.05% for all cases indicating that the solution does not change significantly at higher iterations. Based on this result, it was concluded that 10,000 iterations were adequate to obtain results for all of the simulations.

3.2 Result

3.2.1 Response Surface Model

Seven uncertain closure coefficients and their respective epistemic interval were identified for the turbulence model as mentioned in Section 2.1.1. To generate the response surface model, the

framework as previously described in Section 2.2 was employed. Three outputs of interest were chosen which are the lift and drag coefficients, and the sum of squared errors (SSE) between the chordwise pressure distribution of the experimental data and the numerical computations. The SSE was also used as the system output to determine the calibration of the closure coefficients and for the uncertainty quantification and sensitivity analysis. The procedure of the ADOE is described as followings:

1. The algorithm was initialised with 2^7=128 sample points by a two–level full factorial approach for each angle of attack (128 x 6 α). This initialization is based on the traditional DOE technique.

2. The machine learning technique is then utilised to identify the best candidate design points based on the available results and on a balanced strategy between the space– and feature–learning. The output variables for the new design points are then computed through CFD, and this step is iterated until the maximum number of CFD evaluations is reached. In this study, this step entailed the execution of 100 CFD runs in 10,000 iterations.

3. The best surrogate model was identified automatically by the machine learning algorithm in order to link the seven input variables to the desired output based on table containing a total number of 600 experiments.

In total, 1368 CFD simulations were performed utilizing 456 CPU hours.

Table 2 C_L for three level of grids at α=5.13 deg and Re=$2{\cdot}10^6$.

Grid	C_L	Δ %
Fine	0.7707	5.45
Medium	0.7698	5.57
Coarse	0.7593	6.98
Experiment	0.7430	-

Table 3 The C_L computed for two angles of attack at every intermediate check points at Re=$2{\cdot}10^6$

Iterations	C_L	
	5.13 deg	**11.22 deg**
10,000	0.7698	1.2589
15,000	0.7696	1.2585
20,000	0.7694	1.2585

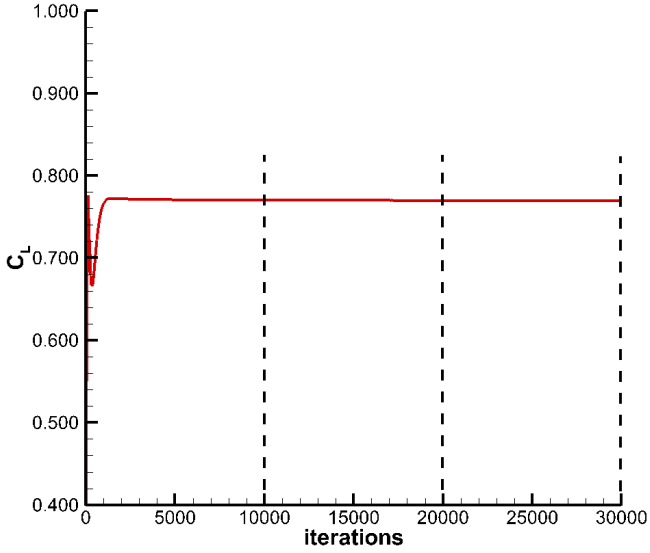

Fig. 3 Convergence of the lift coefficients for the S809 airfoil at α=5.13 deg (Re=$2{\cdot}10^6$).

3.2.2 Coefficients Sensitivity Analysis

One of the initiative employs in this paper is to analyse the sensitivity of the coefficient towards the output of interests. As previously mentioned, the initial intention is to calibrate 7 identified coefficients at 6 angles of attack at similar flow condition. It was found that some of the coefficients particularly the C_{sep} had a larger influence at higher angles of attack, causing fluctuation of the results. The fluctuation of the C_L when C_{sep}

equals to 0 and 1 is depicted in Figs. 4(a) and 4(b).

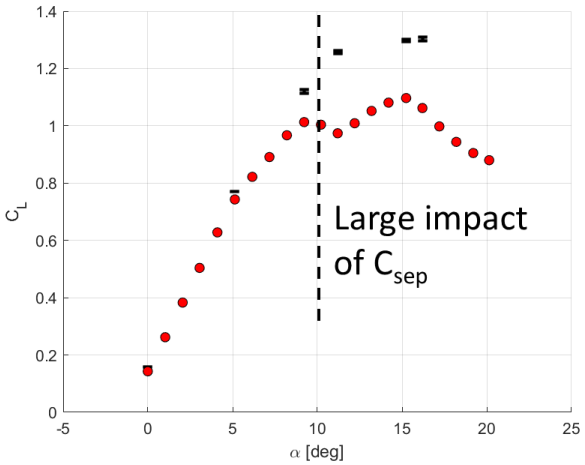

(a) C_{sep}=1

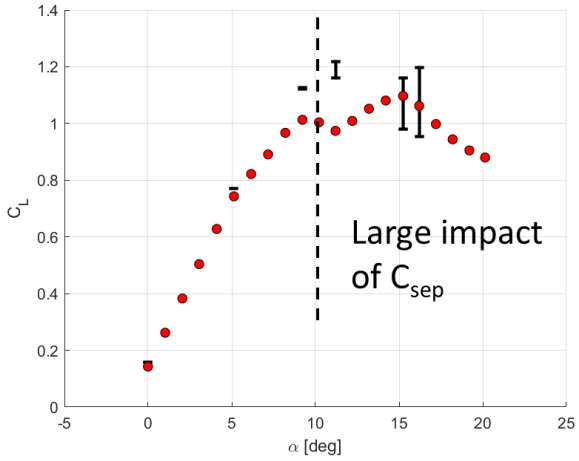

(b) C_{sep}=0

Fig. 4 The fluctuation of C_L for C_{sep} equal to 0 and 1. The error bar denotes the range of the fluctuation at given α.

The observed behavior in these figures can be explained by the influenced of the additional term as in Eq. 4. As the angle of attack is increased, the bubble decreases in length and has almost disappeared at α=5.13 deg [23]. The presence of separation bubble at low angle of attack is controlled by the 'max$(3C_{sep}\mu - \mu_t, 0)$' term, affecting the production of the intermittency around the airfoil as shown in Fig. 5. In this figure, the production of the intermittency is delayed when C_{sep}=1. At higher angle, the turbulent viscosity, μ_t, exceeds the molecular viscosity, μ, hence the additional term should always been switched off. However, by setting the value of C_{sep} to 1, will activates the term hence compromising the reliability of the turbulence model. Although smaller fluctuation is observed, the C_L is overpredicted. Therefore prior knowledge regarding the presence of the separation bubble is necessary to avoid such problem. By considering this behavior, it seems adequate to treat C_{sep} separately from the epistemic variables of the turbulence model. By doing so, it is evident that C_{sep} plays a role at higher angles of attack, affecting greatly the solution convergence.

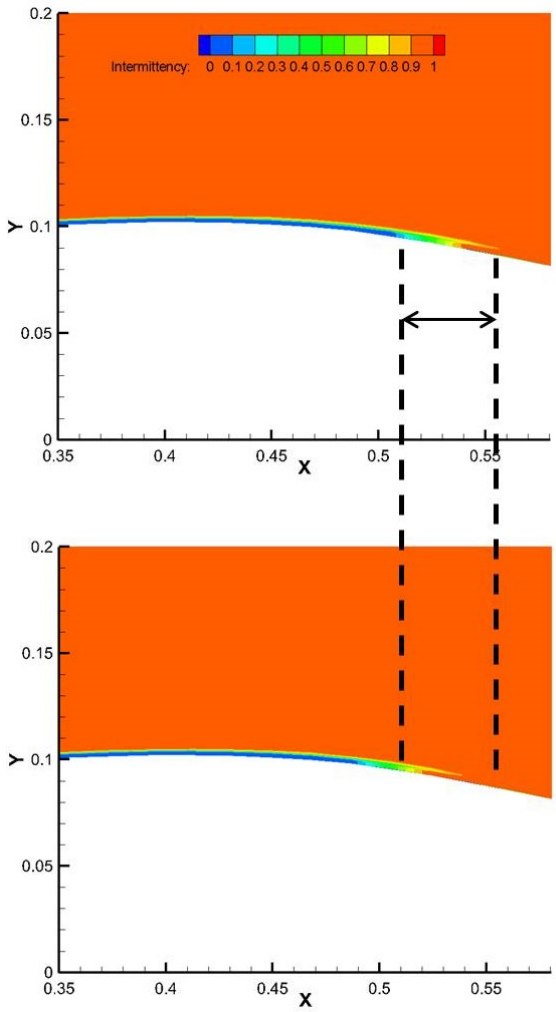

Fig. 5 The fluctuation of C_L for C_{sep} equal to 1 (top) and 0 (bottom) at α=-0.01 deg. The other epistemic variables are assigned to their respective nominal value.

3.2.3 Additional Remarks

Although a significant improvement between the modified and the standard solutions cannot be presented, it was shown that the current initiative can perform an automatic calibration of the closure coefficients. The factors that possibly contributed to this situation are as followings: 1) The success of this sort of work depends on the implementation details of the flow solver such as the limiters. By definition, it limits some quantities within certain bounds. Here in this work, the access to these limiters are limited therefore it restricts the range of changes in the output quantities. This behavior is manifested in Fig. 6. The results appear to be clustered in layers with the same SSE despite all closure coefficients being modified. 2) It is assumed that the experimental data are free from errors, however, this is certainly not the case. The paper therefore demonstrates the possibilities to lead an automatic calibration if accurate experimental data are available.

4 Conclusion

Modelling the transition process is essential to avoid incorrect prediction of the load hence the performance of a wind turbine. However, the coefficients of a turbulence model were designed for generic test cases and contribute to the source of uncertainty in the CFD calculation. To reduce the uncertainty, the turbulence model needed calibration. In this study, this aspect was notably addressed by utilizing multidisciplinary technique including machine–learning method, a flow solver and a high–performance computing facility. Among the findings are: a) selected number of the coefficients have significant influence on the final output of interest, particularly the C_{sep} when separation bubble was observed on the airfoil and b) the accomplishment of this type of work depends on several factors e.g. the solver limiters where it limits the variation of the output quantities. If this condition is met, then the work can be conducted without any constraints.

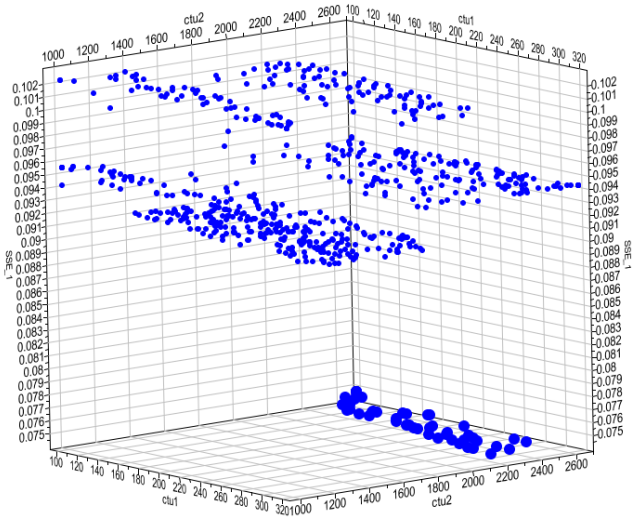

Fig. 6 The clustered results within similar SSE to show the restriction applied on the output quantities by the solver limiters.

References

[1] Cheung SH, Oliver TA, Prudencio EE, Prudhomme S and Moser RD. Bayesian uncertainty analysis with applications to turbulence modeling. *Reliability Engineering & System Safety*, Vol. 96, No. 9, pp 1137-1149, 2011.

[2] Cruz E, Joshi Y, Iyengar M, Schmidt R. Comparison of numerical modeling to experimental data in a small, low power data center test cell. *ASME 2009 International Mechanical Engineering Congress and Exposition*, American Society of Mechanical Engineers, InterPACK 2009-89306, pp 1437-1445, 2009.

[3] Yarlanki S, Rajendran B, Hamann H. Estimation of turbulence closure coefficients for data centers using machine learning algorithms. *Thermal and Thermomechanical Phenomena in Electronic Systems (ITherm)*, IEEE Intersociety Conference, pp 38-42, 2012.

[4] Sørensen NN. CFD modelling of laminar-turbulent transition for airfoils and rotors using the γ-model. *Wind Energy*, Vol. 12, No. 8, pp 715-733, 2019.

[5] Da Ronch A, Panzeri M, Drofelnik J and d'Ippolito R. Data-driven optimisation of closure coefficients of a turbulence model. University of Southampton, doi:10.5258/SOTON/D0263, 2017.

[6] Ansys. *Ansys 17.0 help*. 2016.

[7] Colonia S, Leble V, Steijl R and Barakos G. Assessment and calibration of the γ-equation transition model at low mach. *AIAA Journal*, pp 1126-1139, 2017.

[8] Khayatzadeh P and Nadarajah S. Laminar–turbulent flow simulation for wind turbine profiles using the γ-$Re_{\theta t}$ transition model. *Wind Energy*, Vol. 17, No. 6, pp 901-918, 2014.

[9] Menter FR, Langtry R and Völker S. Transition modelling for general purpose CFD codes. *Flow, Turbulence and Combustion*, Vol. 77, No. 1-4, pp 277-303, 2006.

[10] Menter FR and Langtry RB. Transition modelling for turbomachinery flows. *Low Reynolds Number Aerodynamics and Transition*. Intech, 2012.

[11] Smith AMO and Gamberoni N. Transition, pressure gradient, and stability theory. *Report no. ES.26388*, Douglas Aircraft Co., 1956.

[12] Van Ingen JL. A suggested semi-empirical method for the calculation of the boundary layer transition region. *Technische Hogeschool Delft, Vliegtuigbouwkunde, Rapport VTH-74*, 1956.

[13] Menter FR, Smirnov PE, Liu T and Avancha R. A one-equation local correlation-based transition model. *Flow, Turbulence and Combustion*, Vol. 95, No. 4, pp 583-619, 2015.

[14] Menter FR, Langtry RB, Likki SR, Suzen YB, Huang PG and Völker S. A correlation-based transition model using local variables - part i : model formulation. *Journal of Turbomachinery*, Vol. 128, No. 3, pp. 413-422, 2006.

[15] Langtry RB and Menter FR. Correlation-based transition modeling for unstructured parallelized computational fluid dynamics codes. *AIAA journal*, Vol. 47, No. 12, pp 2894-2906, 2009.

[16] Mayda EA and Van Dam CP. Bubble-induced unsteadiness on a wind turbine airfoil. *Journal of Solar Energy Engineering*, Vol. 124, No. 4, pp 335-344, 2002.

[17] Windte J, Radespiel R, Scholz U and Eisfeld B. RANS Simulation of the Transitional Flow around Airfoils at Low Reynolds Numbers for Steady and Unsteady Onset Conditions. Technical Univ Braunschweig (Germany) Inst of Fluid Mechanics, 2004.

[18] Lian Y and Shyy W. Laminar-turbulent transition of a low reynolds number rigid or flexible airfoil. *AIAA Journal*, Vol. 45, No. 7, pp 1501-1513, 2007.

[19] Da Ronch A, Panzeri M, and Abd Bari MA, d'Ippolito R and Franciolini M. Adaptive design of experiments for efficient and accurate estimation of aerodynamic loads. *Aircraft Engineering and Aerospace Technology*, Vol. 89, No. 4, pp 558-569, 2017. 10.1108/AEAT-10-2016-0173.

[20] Noesis Solutions. *Optimus Rev 10.19 - User's Manual*. 2017.

[21] Abu-Ghannam BJ and Shaw R. Natural transition of boundary layers–the effects of turbulence, pressure gradient, and flow history. *Journal of Mechanical Engineering Science*, Vol. 22, No. 5, pp 213-228, 1980.

[22] Hall, DJ. *Boundary layer transition*. PhD Dissertation, University of Liverpool, 1968.

[23] Somers DM. Design and experimental results for the S809 airfoil. *No. NREL/SR–440-6918*, National Renewable Energy Lab., Golden, CO (United States), 1997.

5 Contact Author Email Address

Corresponding author : M Anas Abd Bari
Email address : Anas.Abd-Bari@soton.ac.uk

Copyright Statement